JCTC Journal of Chemical Theory and Computation

On the Accuracy of Density Functional Theory to Predict Shifts in Nuclear Magnetic Resonance Shielding Constants due to Hydrogen Bonding

Jacob Kongsted*

Department of Theoretical Chemistry, Chemical Center, University of Lund, P.O. Box 124, S-221 00 Lund, Sweden

Kestutis Aidas, Kurt V. Mikkelsen, and Stephan P. A. Sauer

Department of Chemistry, University of Copenhagen, Universitetsparken 5, DK-2100 Copenhagen Ø, Denmark

Received October 25, 2007

Abstract: We present the first systematic investigation of shifts in the nuclear magnetic resonance (NMR) shielding constant due to hydrogen bonding using either the series of wave function based methods, Hartree−Fock (HF), second-order Møller-Plesset perturbation theory (MP2), Coupled Cluster Singles and Doubles (CCSD) and CCSD extended with an approximate description of triples (CCSD(T)), or Density Functional Theory (DFT) employing either the B3LYP, PBE0, or KT3 exchange correlation (*xc*) functionals. The molecular systems considered are (i) the water dimer and (ii) formaldehyde in complex with two water molecules. Specially for the ^{17}O in formaldehyde we observe significant differences between the DFT and CCSD(T) predictions. However, the extent of these deviations depends crucially on the applied *xc* functional. Compared to CCSD(T) we find the KT3 functional to provide accurate results, whereas both B3LYP and PBE0 are in significant error. Potential consequences of this observation are discussed in the context of general predictions of NMR shielding constants in condensed phase.

I. Introduction

Among the intermolecular forces acting between molecules in a condensed medium, the hydrogen bond is by far the strongest and plays in fact an important role when characterizing the chemical nature of a given molecular system. For example, hydrogen bonding is essential in determining the 3D geometries adopted by nucleic bases and proteins. In such large molecules, the hydrogen bonds between different regions within the same macromolecule may cause it to fold and thereby adapt a specific shape which partly determines its biochemical function.[1] In DNA the double helical structure is largely due to specific hydrogen bonding between base pairs, and in proteins hydrogen bonds form between the backbone oxygens and amide hydrogens. Hydrogen bonds are usually classified according to the strength, i.e., strong (> 15 kcal/mol), moderate (4−15 kcal/mol), and weak (< 4 kcal/mol).[2] The strength of a hydrogen bond is closely related to the geometry or bond directionality, i.e., the angle (α) between D−H and H···A, where D and A are the donor and acceptor groups, respectively.[3] The preferable geometry of the hydrogen bond is found[4] for R(H···A) ∼ 2 Å and α in the range from 140° to 180°.

In recent years a lot of research has focused on the ability of DFT to describe the geometry and energetics of hydrogen bonds.[3] DFT is for this application, due to the potential low scaling of this method, an obvious candidate. However, the accuracy of DFT in the description of hydrogen bonds depends strongly on the specific type of *xc* functional employed in the calculation. It has been found that local density approximation (LDA) functionals largely overestimate the strength of hydrogen bonds, while a much better description is provided by using either generalized gradient

* Corresponding author e-mail: Jacob.Kongsted@teokem.lu.se.

10.1021/ct700285j CCC: $40.75
Published on Web 01/16/2008

approximation (GGA) or general hybrid *xc* functionals (see for example the excellent paper by Ireta et al.[3] and references therein).

In contrast to the large amount of data available on the performance of DFT versus high level wave function methods for the geometry and energetics of hydrogen bonds,[3] only little is known about the accuracy of DFT in the calculation of changes in general spectroscopic properties due to the presence of hydrogen bonds in extended systems.[5] Obviously, this is related to the fact that, due to the inherently large size of such systems, great difficulties are encountered when trying to base the quantum chemical description on correlated wave function approaches. However, the question is fundamental and requires attention. This should particularly be seen in light of the fact that DFT is now widely used and has become accepted in calculations of general molecular properties for isolated molecules.

In this paper we will present a systematic investigation of shifts in NMR shielding constants due to hydrogen bonding using either the series of wave function based methods HF, MP2, CCSD, and CCSD(T) or DFT employing either the B3LYP,[6] PBE0,[7,8] or KT3[9] *xc* functionals. We consider either the water dimer or formaldehyde in complex with two water molecules. For these two small model systems we will present a systematic study of the effect of varying the electronic structure method with particular focus on the performance of the DFT based methods as compared to high level wave function methods like CCSD(T). It has previously been established that CCSD(T) is capable of predicting NMR shielding constants very accurately (see for example ref 10), and we will in this study use this model as the theoretical reference. The NMR shielding constants are known to be very sensitive to the chemical environment and specially hydrogen bonding may change the magnitude of the resonance frequency. In addition, it is well-known that NMR spectroscopy is a powerful tool for predicting protein structure and that ab initio calculations can provide important help in assigning experimental NMR spectra.[11,12] It is therefore of both fundamental and practical interest to assess to what extent DFT may be used to predict NMR shielding constants in hydrogen-bonded molecular systems. Even though the molecular systems studied here are relatively small, they are appropriate model systems for more complex samples, e.g., acetone or other carbonyl compounds solvated by water, and bear the important chemistry characteristic for the class of carbonyl compounds. Moreover, these model systems are small enough for accurate quantum chemical methods to be applied. We therefore believe that our findings are of great importance for benchmarking solvent models for quantitative NMR predictions in particular in light of very recent progress within linear scaling methods applied to DFT[13] calculations of NMR shielding constants, which opens the door for quantum chemical calculations of NMR properties on very large and complex chemical systems.

The rest of this paper is organized in the following way. In section II we outline the computational protocol. In section III we first present and discuss the results for the water dimer and then turn to the system composed of formaldehyde and two water molecules. Finally, we end this paper by a discussion presented in section IV.

II. Computational Methods

The theoretical aspects of calculations of NMR shielding tensors are well-known and will not be repeated here. Instead we refer to ref 14 for a general and comprehensive review. Special theoretical aspects of the Coupled Cluster based calculations may be found in refs 15−18, whereas calculations of NMR shielding constants based on DFT are described in refs 19−23.

The molecular geometries of water and the water dimer were optimized using CCSD(T), whereas the geometries of formaldehyde and formaldehyde complexed with two water molecules were optimized using CCSD. In all cases we used the aug-cc-pVTZ basis set.[24] In all calculations the frozen core consisted of the 1s orbitals on the heavy atoms. The geometry optimizations were performed using the Dalton Quantum Chemistry Program.[25] The calculations of the NMR shielding constants at the HF, MP2, and CC level of theory were performed using the Mainz-Austin-Budapest version of ACES II.[26,27] The CC calculations were run either at the CCSD or the CCSD(T) level of theory. In the property calculations based on MP2 or CC all electrons were correlated. The calculations based on DFT were carried out with the Dalton[25] program employing either the B3LYP,[6] PBE0,[7,8] or the KT3[9] *xc* functionals. The B3LYP and PBE0 are general hybrid functionals, whereas KT3 belongs to the group of GGA *xc* functionals. KT3 has been designed with the specific aim of providing high quality NMR shielding constants for light, main-group nuclei.[9] This has been accomplished by an increase in the HOMO−LUMO gap. We emphasize however that no environmental effects have been considered in the parametrization of the KT3 *xc* functional. Using the PBE0 *xc* functional we have considered basis set superposition errors using the counterpoise approach.[28] In order to ensure origin-independent results for the NMR shielding constants, we use Gauge Including Atomic Orbitals.[29−33] In this work we only consider isotropic NMR shielding constants.

III. Results and Discussion

In this section we will present the results of the calculations described in the preceding section. We begin by discussing the results obtained for isolated water and the water dimer and then continue to discuss the case of formaldehyde and the complex of formaldehyde with two water molecules.

A. Water. *1. Basis Set Analysis*. In Table 1 we present a basis set analysis for the NMR isotropic shielding constants $\sigma(^1\mathrm{H})$ and $\sigma(^{17}\mathrm{O})$ for the isolated water molecule. The calculations refer to CCSD(T) and various basis sets. As seen from Table 1 a reasonably fast basis set convergence is achieved when increasing the cardinal number (X) within the correlation consistent series of the aug-cc-pVXZ basis sets. The inclusion of the tight core functions in the aug-cc-pCVXZ basis sets is seen only to have an effect for the lowest cardinal number, i.e., X=D(2). In addition to the basis set analysis for the isolated water molecule, we present in Table 2 corresponding results for the water dimer (see Figure

Table 1. $\sigma(^1H)$ and $\sigma(^{17}O)$ NMR Isotropic Shielding Constants of Water (CCSD(T)/aug-cc-pVTZ Optimized Geometry) Calculated Using CCSD(T) and Various Basis Sets[a]

basis	$\sigma(^1H)$	$\sigma(^{17}O)$
aug-cc-pVDZ	31.41	344.46
aug-cc-pCVDZ	31.39	342.79
aug-cc-pVTZ	30.89	336.67
aug-cc-pCVTZ	30.87	336.55
aug-cc-pVQZ	30.60	336.54
aug-cc-pCVQZ	30.59	336.15

[a] Results are in units of ppm.

Table 2. $\sigma(^1H)$ and $\sigma(^{17}O)$ NMR Isotropic Shielding Constants of Selected Nuclei in the Water Dimer (CCSD(T)/aug-cc-pVTZ Optimized Geometry) Calculated Using CCSD and Various Basis Sets[a]

basis	$\sigma(^1H4)$	$\sigma(^{17}O1)$	$\sigma(^{17}O2)$
aug-cc-pVDZ	28.45	340.63	337.25
aug-cc-pCVDZ	28.43	338.98	335.47
aug-cc-pVTZ	27.92	332.80	328.63
aug-cc-pCVTZ	27.90	332.54	328.58
aug-cc-pVQZ	27.58	332.36	328.59

[a] Results are in units of ppm. See Figure 1 for the atom labeling.

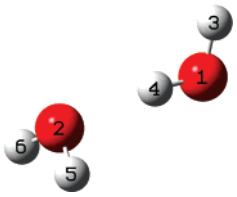

Figure 1. Atom labeling in the water dimer. (1,3,4) − proton donor, (2,5,6) − proton acceptor.

1 for the atom labeling). Due to computational demands the latter basis set analysis has been restricted to the CCSD level of theory. From Table 2 we observe the same trends as found from the calculation on the isolated water molecule, i.e., the NMR isotropic shielding constants are well converged using the aug-cc-pVTZ basis set. Based on the results presented in Tables 1 and 2, the aug-cc-pVTZ basis set was chosen for the rest of the calculations presented here for water and the water dimer.

2. Shifts in NMR Shielding Constants due to Hydrogen Bonding. Having found an appropriate basis set for the NMR shielding constant calculations, we now proceed to consider selected isotropic NMR shielding constants in the water dimer. Figure 1 shows the orientation of the individual water molecules within the dimer. In addition, it defines the atomic labels used in the following. The atoms 1, 3, and 4 constitute the proton donor, whereas the atoms 2, 5, and 6 define the proton acceptor. In the following we will restrict ourselves to consider atoms directly involved in the formation of the hydrogen bond, that is, atoms labeled 1, 2, and 4. For these atoms the absolute values of the isotropic NMR shielding constants are presented in Table 3. In addition, we have also included the results obtained for the isolated proton donor or acceptor using the same internal geometries as in the water dimer as well as the results for the isolated geometry optimized water monomer. For the $\sigma(^{17}O)$ we generally observe a good agreement between CCSD and CCSD(T), whereas the DFT based methods and HF tend to underestimate the shielding constants. On the other hand, the use of MP2 leads to overestimated results. At the CCSD(T) level of theory the difference in the donor−acceptor $\sigma(^{17}O)$ amounts to around 4 ppm. Keeping the internal geometries of the water molecules, but otherwise treating them as isolated species, changes the same difference to around −1 ppm. We thereby observe that geometrical and polarization effects are in opposite directions. On average, the PBE0 functional is seen to perform slightly better than B3LYP or KT3, but the improvement is in any case small.

For $\sigma(^1H)$ the inclusion of approximate triples is seen to have an almost negligible effect as compared to CCSD. In contrast to $\sigma(^{17}O)$ both HF and MP2 now tend to underestimate the results, whereas the DFT based methods now give overestimated results with respect to CCSD(T) although the changes are much smaller than that found for $\sigma(^{17}O)$.

Turning now to the core of this paper, we present DFT and wave function based results for the shifts in NMR shielding constants in Tables 4 and 5, respectively. In the following we will denote shifts due to hydrogen bonding by Δ. The shifts termed "Frozen" are calculated using the dimer geometry of the individual water molecules, whereas the shifts termed "Relaxed" are computed with respect to the isolated geometry optimized water molecule. The relaxed shifts are always more negative, i.e., the absolute values are larger than the corresponding frozen shifts. As seen from Table 4 only small deviations are found between the different *xc* functionals even though B3LYP seems to provide slightly larger magnitudes of the shifts. The BSSE corrected results based on the PBE0 *xc* functional are also listed in Table 4. Here we observe that the effect of BSSE is very small amounting to only around 2% of the total frozen shift for O2 and vanishes for H4 (i.e., the atoms defining the hydrogen bond). It has previously been stated that the effect of BSSEs are handled in an effective way using large and flexible basis sets including diffuse basis functions[34] which also is reflected by our findings. Comparing the shifts obtained with DFT to the corresponding results from the wave function calculations, we find a general decrease in the magnitude of the shifts. This is illustrated in Figure 2 which shows the "Frozen" and "Relaxed" $\Delta\sigma(^1H4)$, $\Delta\sigma(^{17}O2)$, and $\Delta\sigma(^{17}O1)$ shifts for atoms in the water dimer with respect to the CCSD(T) predictions. Note that for O2 and H4 the HF model is found to provide surprisingly good results, whereas this model completely fails for O1. For this specific molecular system KT3 and PBE0 are seen to perform better than B3LYP, but no general improvement is seen on going from PBE0 to KT3.

In order to explore potential differences between the performance of PBE0 and KT3 in more detail, we have performed a series of calculations with varying lengths and angles of the hydrogen bond. In Figure 3 we have plotted the difference between the shifts due to hydrogen bonding in the NMR shielding constants for O2 obtained using PBE0 or KT3 and CCSD(T) as a function of the distance between the two oxygen atoms in the water dimer. The intramolecular

Table 3. $\sigma(^1H)$ and $\sigma(^{17}O)$ NMR Isotropic Shielding Constants of Water and the Water Dimer Calculated Using Various Electronic Structure Methods in Combination with the aug-cc-pVTZ Basis Set[a]

	atom	site	B3LYP	PBE0	KT3	HF	MP2	CCSD	CCSD(T)
water dimer	O	1	322.09	324.64	322.93	326.08	340.04	332.80	333.27
	O	2	316.86	319.93	317.44	319.10	336.98	328.63	329.39
	H	4	28.08	28.02	28.46	27.52	27.75	27.92	27.95
proton donor	O	1	324.58	327.04	324.53	325.14	343.49	334.49	335.37
	H	4	30.92	30.82	31.23	30.34	30.38	30.63	30.65
proton acceptor	O	2	325.59	328.01	325.55	326.11	344.24	335.36	336.23
water monomer	O		326.09	328.50	326.05	326.58	344.64	335.80	336.67
	H		31.15	31.05	31.46	30.59	30.63	30.87	30.89

[a] Results are in units of ppm. See Figure 1 for the atom labeling.

Table 4. $\Delta\sigma(^1H)$ and $\Delta\sigma(^{17}O)$ for the Atoms in the Water Dimer Computed Using DFT[a]

		B3LYP		PBE0		PBE0 (BSSE)	KT3	
atom	site	frozen	relaxed	frozen	relaxed	frozen	frozen	relaxed
O	1	−2.49	−4.00	−2.40	−3.86	−2.55	−1.60	−3.12
O	2	−8.73	−9.23	−8.08	−8.57	−7.87	−8.11	−8.61
H	4	−2.84	−3.07	−2.80	−3.03	−2.80	−2.77	−3.00

[a] The shifts termed "Frozen" are calculated using the in-dimer geometry of the individual water molecules, whereas the shifts termed "Relaxed" are computed with respect to the isolated geometry optimized water molecule. The results indicated by PBE0(BSSE) have been corrected for BSSE. All molecular geometries have been optimized using CCSD(T)/aug-cc-pVTZ. Results are in units of ppm. See Figure 1 for the atom labeling.

Table 5. $\Delta\sigma(^1H)$ and $\Delta\sigma(^{17}O)$ for the Atoms in the Water Dimer Computed Using Various Wave Function Methods[a]

		HF		MP2		CCSD		CCSD(T)	
atom	site	frozen	relaxed	frozen	relaxed	frozen	relaxed	frozen	relaxed
O	1	0.94	−0.50	−3.45	−4.60	−1.69	−3.00	−2.10	−3.40
O	2	−7.01	−7.48	−7.26	−7.66	−6.73	−7.17	−6.84	−7.28
H	4	−2.82	−3.07	−2.63	−2.88	−2.71	−2.95	−2.70	−2.94

[a] The shifts termed "Frozen" are calculated using the in-dimer geometry of the individual water molecules, whereas the shifts termed "Relaxed" are computed with respect to the isolated geometry optimized water molecule. All molecular geometries have been optimized using CCSD(T)/aug-cc-pVTZ. Results are in units of ppm. See Figure 1 for the atom labeling.

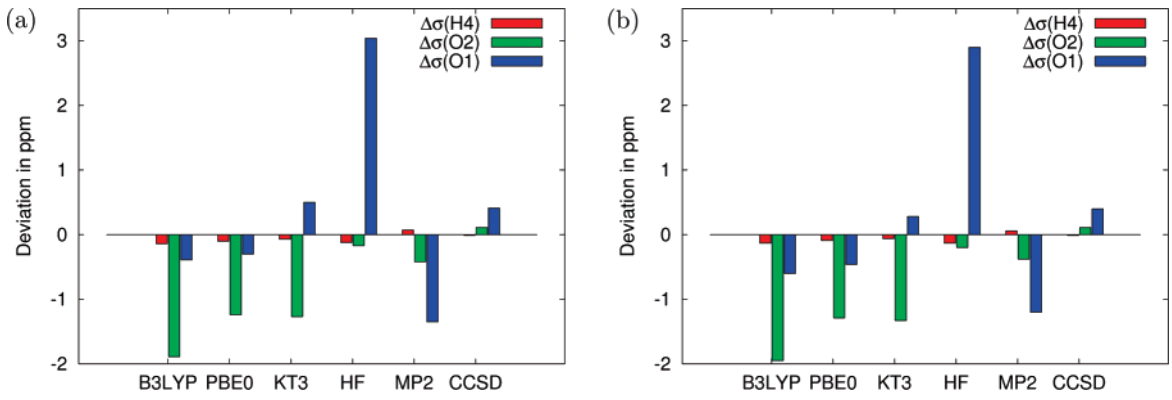

Figure 2. (a) Frozen and (b) Relaxed shifts $\Delta\sigma(^1H4)$, $\Delta\sigma(^{17}O2)$, and $\Delta\sigma(^{17}O1)$ for the atoms in the water dimer with respect to the corresponding CCSD(T) predictions. See Figure 1 for the atom labeling.

geometries of the individual water molecules have been kept frozen. From this figure we observe that results obtained using these two different *xc* functionals begin to diverge at O1−O2 separations shorter than the equilibrium geometry (2.914 Å). At O1−O2 distances within the range of the equilibrium values, the KT3 *xc* functional is seen to perform better than PBE0, i.e., it has smaller deviations with respect to the CCSD(T) predictions. A similar conclusion can be drawn from a set of similar calculations where now the hydrogen bond angle is changed. This is illustrated in Figure 4 which shows the difference between the shifts due to hydrogen bonding in the NMR shielding constants for O2 obtained using PBE0 or KT3 and CCSD(T) as a function of the deviation in the O1−H4−O2 angle with respect to the equilibrium geometry. The O1−H4−O2 angle in the equilibrium geometry is 171.6°. For very small changes in this angle, KT3 and PBE0 perform similarly, but for larger deviations KT3 tends to provide results in better agreement with CCSD(T). An important observation from Figure 4 is that the error, relative to CCSD(T), introduced using the KT3

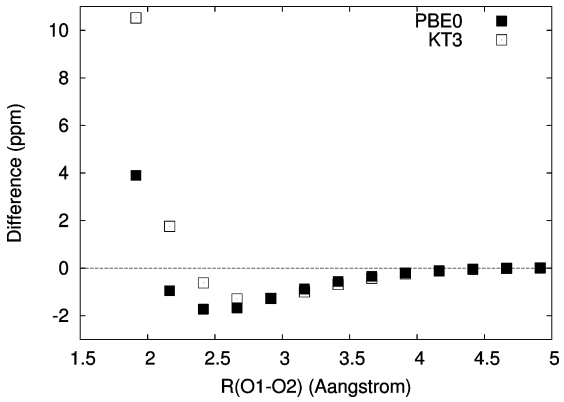

Figure 3. The intrinsic difference between DFT (PBE0 or KT3) and CCSD(T) with respect to the effect of hydrogen bonding on the isotropic NMR shielding constant of O2 (defined according to Figure 1) as a function of the distance between the two oxygen atoms in the water dimer. The intramolecular geometries of the individual water molecules have been kept frozen. The difference is defined as $\Delta\sigma^{O2}_{DFT}(R) - \Delta\sigma^{O2}_{CC}(R)$. The equilibrium distance in the water dimer is $R = 2.914$ Å. The basis set used is the aug-cc-pVTZ basis set.

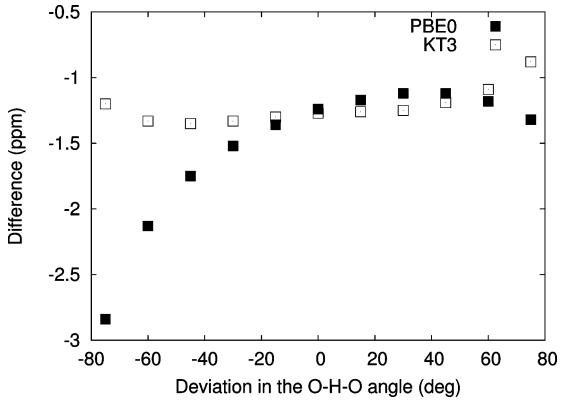

Figure 4. The intrinsic difference between DFT (PBE0 or KT3) and CCSD(T) with respect to the effect of hydrogen bonding on the isotropic NMR shielding of O2 (defined according to Figure 1) in the water dimer as a function of the deviation in the O1−H4−O2 angle (Θ) with respect to the equilibrium geometry. The intramolecular geometries of the individual water molecules have been kept frozen. The difference is defined as $\Delta\sigma^{O2}_{DFT}(\Theta) - \Delta\sigma^{O2}_{CC}(\Theta)$. The O1−H4−O2 angle in the equilibrium geometry is 171.6°. The basis set used is the aug-cc-pVTZ basis set.

xc functional is almost constant in a significant range. This is important since accurate models used to predict solvent effects on NMR shielding constants rely on a sampling over different solute−solvent configurations. For such a method to be valid it is important that the error in each calculation reflecting a specific configuration should be as constant as possible (and ideally equal to zero). Based on this reason we conclude that the most reliable *xc* functional to be considered in use for calculation of NMR shielding constants for systems like liquid water is likely to be KT3.

B. Formaldehyde. Having discussed the results for water and the water dimer we now turn to the case of formaldehyde and formaldehyde complexed with two water molecules.

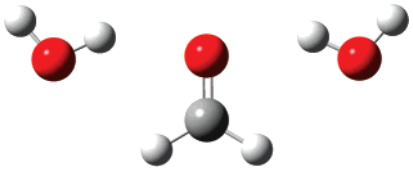

Figure 5. The hydrogen-bonded complex of formaldehyde and two water molecules as optimized using CCSD/aug-cc-pVTZ.

Table 6. $\sigma(^{13}C)$ and $\sigma(^{17}O)$ NMR Isotropic Shielding Constants of Formaldehyde Calculated Using CCSD[a]

basis	$\sigma(^{13}C)$	$\sigma(^{17}O)$
aug-cc-pVDZ	29.25	−300.68
aug-cc-pCVDZ	24.78	−311.92
aug-cc-pVTZ	11.77	−354.20
aug-cc-pCVTZ	8.09	−363.60
aug-cc-pVQZ	6.02	−367.46
aug-cc-pCVQZ	3.74	−372.83
aug-cc-pV5Z	3.10	−374.52

[a] The geometry used has been obtained from CCSD/aug-cc-pVTZ geometry optimization. Results are in units of ppm.

Apart from a purely academic point of view this system is interesting since formaldehyde is the smallest carbonyl compound thereby bearing the important chemistry of this class of systems. The structure of the complex of formaldehyde and 2 water molecules is illustrated in Figure 5. The complex possesses an overall C_{2v} symmetry.

1. Basis Set Analysis. In Table 6 we present a basis set analysis for the NMR isotropic shielding constants $\sigma(^{13}C)$ and $\sigma(^{17}O)$ of the isolated formaldehyde molecule. The calculations refer to CCSD and various basis sets and the geometry has been obtained from CCSD/aug-cc-pVTZ geometry optimization. As seen in Table 6, it is extremely difficult to get the shielding constants of formaldehyde converged. Thus, a significant change in shielding constant is observed on increasing the cardinal number from D(2) to T(3). But even when using the aug-cc-pV5Z basis set the results are not yet converged. For $\sigma(^{13}C)$ this very slow basis set convergence has already been observed previously.[10] However, in the present study our main interest is more in the effects induced by hydrogen bonds which means that we have to perform two separate calculations: one with and another without the hydrogen-bonding water molecules. Thereby, one could expect that, due to intrinsic error cancellation in the calculation of the shifts, converged results could be obtained using basis sets of modest size. In Table 7 we present results for the shifts due to hydrogen bonding (Δ) on the $\sigma(^{13}C)$ and $\sigma(^{17}O)$ NMR isotropic shielding constants of formaldehyde calculated using MP2. In addition we also list the absolute values of the shielding constants obtained for the isolated molecule or within the complex. In case of different basis sets used on formaldehyde or water, the nomenclature follows formaldehyde/water. From Table 7 we observe that even though the $\Delta\sigma(^{13}C)$ is rather constant through the series of different basis sets, $\Delta\sigma(^{17}O)$ changes significantly on increasing the cardinal number from D(2) to T(3). However, this is mainly due to the basis functions attached to formaldehyde as can be seen from the calculation

Table 7. $\sigma(^{13}C)$ and $\sigma(^{17}O)$ NMR Isotropic Shielding Constants of Formaldehyde Calculated Using MP2[a]

	complex		monomer		induced	
basis	$\sigma(^{13}C)$	$\sigma(^{17}O)$	$\sigma(^{13}C)$	$\sigma(^{17}O)$	$\Delta\sigma(^{13}C)$	$\Delta\sigma(^{17}O)$
aug-cc-pVDZ	19.47	−217.31	28.22	−267.74	−8.75	50.43
aug-cc-pCVDZ	14.64	−228.33	23.52	−279.42	−8.88	51.09
aug-cc-pVTZ	1.00	−269.29	9.91	−325.28	−8.91	55.99
aug-cc-pCVTZ	−3.19	−277.84	5.94	−335.43	−9.13	57.59
aug-cc-pVTZ/aug-cc-pVDZ	1.02	−270.38	9.91	−325.28	−8.89	54.90
aug-cc-pVQZ/aug-cc-pVDZ	−5.15	−282.03	3.92	−338.50	−9.07	56.47

[a] In case of different basis sets used on formaldehyde or water the nomenclature follows formaldehyde/water. Results are in units of ppm.

Table 8. $\sigma(^{13}C)$ and $\sigma(^{17}O)$ NMR Isotropic Shielding Constants of Formaldehyde Calculated Using CCSD or CCSD(T)[a]

		complex		monomer		induced	
method	basis	$\sigma(^{13}C)$	$\sigma(^{17}O)$	$\sigma(^{13}C)$	$\sigma(^{17}O)$	$\Delta\sigma(^{13}C)$	$\Delta\sigma(^{17}O)$
CCSD	aug-cc-pVDZ	17.17	−248.61	25.73	−321.58	−8.56	72.97
	aug-cc-pVTZ/aug-cc-pVDZ	−0.88	−299.83	7.80	−376.85	−8.68	77.02
CCSD(T)	aug-cc-pVDZ	18.57	−248.31	26.93	−319.44	−8.36	71.13
	aug-cc-pVTZ/aug-cc-pVDZ	0.79	−298.68	9.31	−372.85	−8.52	74.17

[a] Results are in units of ppm.

Table 9. $\sigma(^{13}C)$ and $\sigma(^{17}O)$ NMR Isotropic Shielding Constants of Formaldehyde[a]

	atom	B3LYP	PBE0	KT3	HF	MP2	CCSD	CCSD(T)
$H_2CO + 2H_2O$	O	−362.57	−361.18	−294.36	−336.45	−270.38	−299.83	−298.68
	C	−28.63	−25.62	−4.14	−13.91	1.02	−0.88	0.79
H_2CO frozen	O	−451.96	−452.77	−366.06	−446.37	−325.28	−376.85	−372.85
	C	−19.53	−16.51	3.98	−5.78	9.91	7.80	9.31
H_2CO relaxed	O	−426.17	−426.87	−343.87	−419.03	−306.17	−354.20	−350.63
	C	−14.95	−11.97	7.64	−0.16	13.08	11.77	12.99

[a] The basis set used is aug-cc-pVTZ/aug-cc-pVDZ. Results are in units of ppm.

with the aug-cc-pVDZ basis set on water and the aug-cc-pVTZ basis set on formaldehyde, whose results are only slightly changed compared to the results with the aug-cc-pVTZ basis sets on all atoms in the complex. On the other hand, the results for the shift obtained using the mixed aug-cc-pVTZ/aug-cc-pVDZ basis set are to be considered fairly converged as clearly can be seen from the fact that increasing the cardinal number in the basis set used on formaldehyde from T(3) to Q(4) only changes $\Delta\sigma(^{13}C)$ by around −0.2 ppm and $\Delta\sigma(^{17}O)$ by 1.5 ppm. Including tight core functions in the basis set only gives rise to similar small changes. If not stated differently in the following we will thereby use the mixed aug-cc-pVTZ/aug-cc-pVDZ basis set, that is, aug-cc-pVTZ basis on formaldehyde and aug-cc-pVDZ basis on the water molecules complexing formaldehyde.

To illustrate the effect of further electron correlation we present in Table 8 the corresponding results as reported in Table 7 but employing a higher level of correlation, i.e., using CCSD or CCSD(T). Two basis sets have been used, i.e., the aug-cc-pVDZ and the mixed aug-cc-pVTZ/aug-cc-pVDZ basis sets. Compared to MP2, we observe that the magnitude of $\Delta\sigma(^{13}C)$ is slightly decreased, whereas correlation affects $\Delta\sigma(^{17}O)$ to a much higher level. Thus, using the mixed basis set and changing from MP2 to CCSD leads to an increase in $\Delta\sigma(^{17}O)$ of around 22 ppm, whereas including effects of triples excitations as described by CCSD(T) reduces this increase by about 3 ppm. We thereby already at this stage find that different levels of electronic correlation may affect the computed shifts of NMR shielding constants significantly.

2. Shifts in NMR Shielding Constants due to Hydrogen Bonding. In Table 9 we report the absolute $\sigma(^{13}C)$ and $\sigma(^{17}O)$ NMR isotropic shielding constants of formaldehyde obtained either in the complex with two water molecules (first entry), for isolated formaldehyde employing the in-complex geometry (second entry) or for isolated geometry optimized formaldehyde (third entry). In the property calculations we have used the mixed aug-cc-pVTZ/aug-cc-pVDZ basis set. As seen from Table 9, geometry relaxation of formaldehyde influences the results significantly. For example, at the CCSD(T) level of theory this effect amounts to around 22 ppm for $\sigma(^{17}O)$. The main changes in geometry of formaldehyde upon complexation with two water molecules is an increase in the *CO* bond length. The effect of variations in the *CO* bond length in carbonyl compounds on the $\sigma(^{17}O)$ NMR isotropic shielding constants have previously been considered[39,40] and found to be significant. In general terms we observe from Table 9 that the use of the B3LYP and PBE0 *xc* functionals provide results in reasonable agreement with each other but far from the CCSD(T) predictions. In fact, the magnitude of the B3LYP and PBE0 results is too large which is mainly due to the well-known tendency of DFT to overestimate the paramagnetic contribution to the shielding constants (see for example the discussion in ref 35). However, this artifact is removed by employing the KT3 *xc* functional, which is now seen to provide results in significantly better agreement with CCSD(T). Even the sign of the absolute $\sigma(^{13}C)$ shielding constant, which is predicted wrong by B3LYP and PBE0, is now in agreement with

Table 10. $\Delta\sigma(^{13}C)$ and $\Delta\sigma(^{17}O)$ for the Atoms in the Formaldehyde Computed Using DFT[a]

	B3LYP		PBE0		PBE0(BSSE)	KT3	
atom	frozen	relaxed	frozen	relaxed	frozen	frozen	relaxed
O	89.39	63.6	91.59	65.69	92.05	71.70	49.51
C	−9.10	−13.68	−9.11	−13.65	−9.15	−8.12	−11.78

[a] The shifts termed "Frozen" are calculated using the formaldehyde geometry as in its complex with two water molecules, whereas the shifts termed "Relaxed" are computed with respect to the isolated geometry optimized formaldehyde molecule. The results indicated by PBE0(BSSE) have been corrected for BSSE. Results are in units of ppm.

Table 11. $\Delta\sigma(^{13}C)$ and $\Delta\sigma(^{17}O)$ for the Atoms in Formaldehyde Computed Using Various Wave Function Methods[a]

	HF		MP2		CCSD		CCSD(T)	
atom	frozen	relaxed	frozen	relaxed	frozen	relaxed	frozen	relaxed
O	109.92	82.58	54.90	35.79	77.02	54.37	74.17	51.95
C	−8.13	−13.75	−8.89	−12.06	−8.68	−12.65	−8.52	−12.20

[a] The shifts termed "Frozen" are calculated using the formaldehyde geometry as in its complex with two water molecules, whereas the shifts termed "Relaxed" are computed with respect to the isolated geometry optimized formaldehyde molecule. Results are in units of ppm.

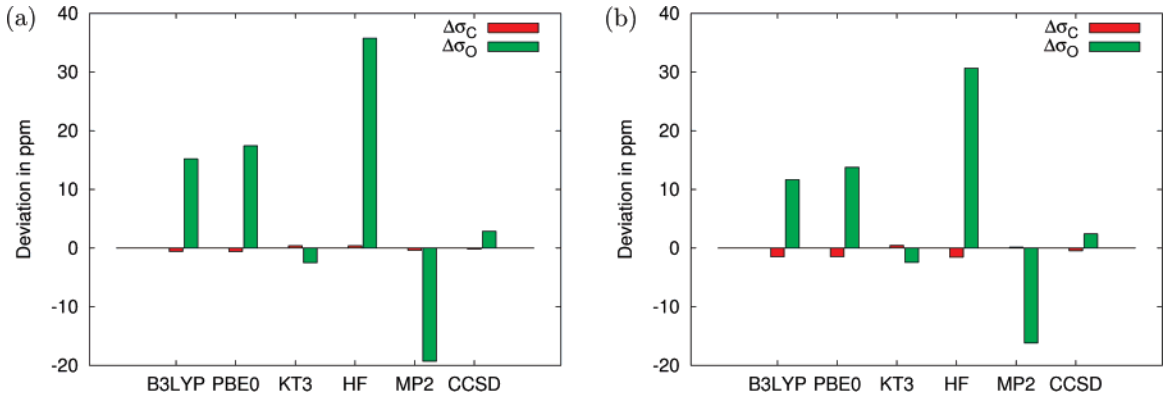

Figure 6. (a) Frozen and (b) Relaxed $\Delta\sigma(^{13}C)$ and $\Delta\sigma(^{17}O)$ for the atoms in formaldehyde with respect to the corresponding CCSD(T) predictions.

CCSD(T). Concerning the wave function based methods, HF gives exaggerated results even though the HF predictions for the absolute shielding constants show a slight improvement as compared to B3LYP and PBE0. For MP2, on the other hand, we generally observe good agreement for $\sigma(^{13}C)$, as compared to CCSD(T), but the MP2 predictions for $\sigma(^{17}O)$ tend to be underestimated. Thereby, the HF and MP2 results are found to be placed opposite relative to the CCSD(T) predictions. The CCSD results are generally close to the CCSD(T) predictions. In summary we find that the KT3 *xc* functional gives results of near CC quality for $\sigma(^{17}O)$, whereas it is slightly less successful in predicting $\sigma(^{13}C)$ confirming earlier findings for small molecules.[23]

Turning now to the effect of the hydrogen bonds on the NMR shielding constants we present in Tables 10 and 11 results based on either DFT (Table 10) or wave function theory (Table 11). As for the water dimer we have included shifts with respect to either a relaxed or frozen (using the in-complex geometry) isolated formaldehyde molecule. For PBE0 we have also included results taking into account the BSSE. Here we find, as for the water dimer, that this only affects the shifts slightly, i.e., around 0.5 ppm for ^{17}O and 0.04 ppm for ^{13}C. As for the case of the absolute NMR shielding constants, we observe from Table 10 a marked difference in the performance of KT3 versus B3LYP or PBE0. The shifts obtained using B3LYP or PBE0 are always larger in magnitude as compared to the KT3 results, i.e., using KT3 instead of either B3LYP or PBE0 reduces the magnitude of the frozen $\Delta\sigma(^{17}O)$ and $\Delta\sigma(^{13}C)$ shifts around 18 and 1 ppm, respectively. However, the KT3 shifts are in very good agreement with the results based on CC and specially CCSD(T). Thus we find also for the shift a very good agreement between DFT/KT3 and CCSD(T). The same observation is found for the relaxed shifts. From Table 11 we observe that even though the MP2 results for $\Delta\sigma(^{13}C)$ are in good agreement with CCSD(T), the corresponding MP2 predictions of $\Delta\sigma(^{17}O)$ are severely underestimated. We are thereby left with the conclusion that, for the $\Delta\sigma(^{17}O)$, B3LYP and PBE0 overestimate the shift due to hydrogen bonding, whereas MP2 severely underestimates this quantity. The many-body electronic structure methods are found to provide results for $\Delta\sigma(^{17}O)$ according to

$$\text{HF} > \text{B3LYP} \simeq \text{PBE0} > \text{CCSD} \simeq \text{CCSD(T)} \simeq \text{KT3} > \text{MP2}$$

For $\Delta\sigma(^{13}C)$, on the other hand, all methods give reasonable results although B3LYP and PBE0 tend to overestimate slightly the effect of the water molecules. This is illustrated in Figure 6 where we have plotted the error in the shift in the NMR shielding constants relative to CCSD(T).

As for the water dimer, further potential differences between the performance of B3LYP/PBE0 and KT3 may be explored by varying the effect of the hydrogen bond strength. This may be done, for example, by changing the length or the angle of the hydrogen bond. In Figure 7 we

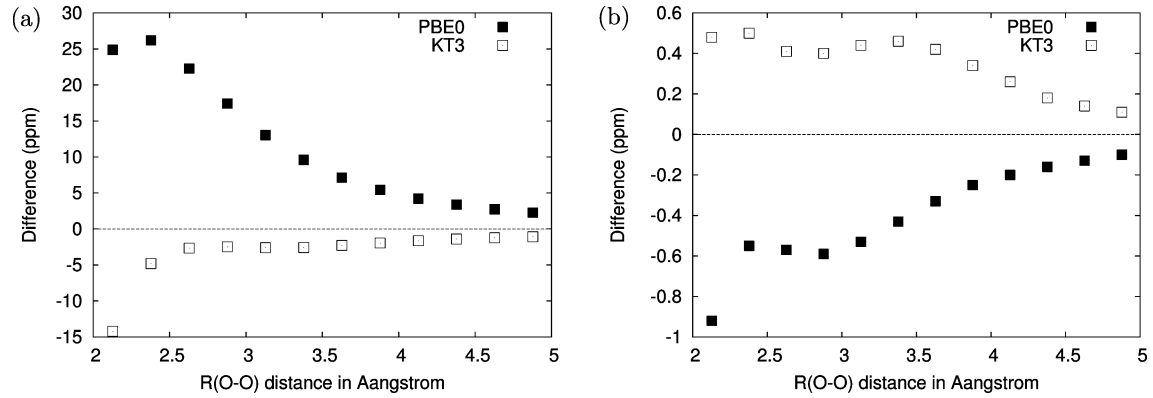

Figure 7. The intrinsic difference between DFT (PBE0 or KT3) and CCSD(T) with respect to the effect of hydrogen bonding on the isotropic NMR shielding constant of the (a) oxygen or (b) carbon atoms in formaldehyde as a function of the distance between the water and formaldehyde oxygen atoms. The water molecules have been displaced symmetrically, and the intramolecular geometries of the individual water molecules have been kept frozen. The difference is defined as $\Delta\sigma^X_{DFT}(R) - \Delta\sigma^X_{CC}(R)$ (X=C,O). The equilibrium distance is $R = 2.878$ Å.

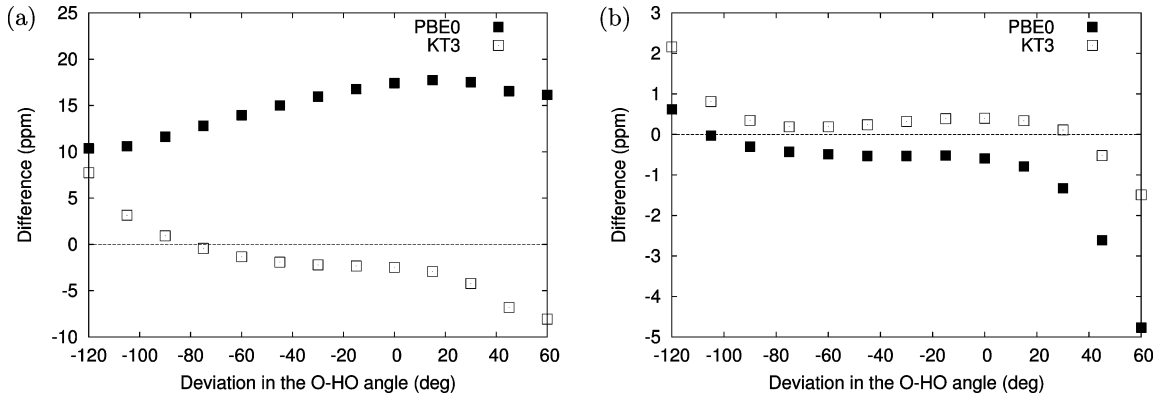

Figure 8. The intrinsic difference between DFT (PBE0 or KT3) and CCSD(T) with respect to the effect of hydrogen bonding on the isotropic NMR shielding constant of the (a) oxygen or (b) carbon atoms in formaldehyde as a function of the deviation in the O−HO angle (Θ) with respect to the equilibrium geometry. This angle is defined as O(formaldehyde)−HO(water) and is in the equilibrium geometry equal to 144.5°. The difference is defined as $\Delta\sigma^X_{DFT}(\Theta) - \Delta\sigma^X_{CC}(\Theta)$ (X=C,O). The intramolecular geometries of the individual water molecules have been kept frozen.

have plotted the intrinsic difference between the DFT (PBE0 or KT3) and CCSD(T) isotropic NMR shielding constant of the oxygen (a) or carbon (b) atoms in formaldehyde as a function of the distance between the water and formaldehyde oxygen atoms. The water molecules have been displaced symmetrically, and the intramolecular geometries of the individual water molecules have been kept frozen. The equilibrium distance is $R = 2.878$ Å. From this figure we observe that the use of the KT3 *xc* functional generally leads to smaller errors as introduced by using the PBE0 *xc* functional. In addition, for KT3 this error is relatively constant over a wider range as compared to PBE0. The potential advantages of this observation are the same as discussed for the water dimer. A similar conclusion can be drawn from a set of calculations where the hydrogen bond angle is changed. This is illustrated in Figure 8 which shows the intrinsic difference between DFT (PBE0 or KT3) and CCSD(T) isotropic NMR shielding constant of the oxygen (a) or carbon (b) atoms in formaldehyde as a function of the deviation in the O−HO angle with respect to the equilibrium geometry. This angle is defined as O(formaldehyde)−HO(water) and is in the equilibrium geometry equal to 144.5°. The intramolecular geometries of the individual water molecules have been kept frozen. From this figure we again observe not only that KT3 provides results for the shift due to hydrogen bonding with a smaller error but also that this error stays relatively constant over a wide range in the hydrogen bond angle. Thus we have clearly shown the advantages of using the KT3 *xc* functional in calculations of NMR shielding constants. Furthermore, according to our findings KT3 should provide both absolute and hydrogen bond induced shifts in the NMR shielding constants at the same accuracy obtained from use of high level wave function based methods, e.g., CCSD(T).

We end this section by a discussion concerning the origin of the observed shifts in NMR shielding constants due to hydrogen bonding. We will only consider the case of formaldehyde in complex with two water molecules and focus on the effect of the hydrogen bond length on $\sigma(^{17}O)$. The effect due to the two water molecules on the NMR shielding constant may generally be divided into electrostatic and nonelectrostatic intermolecular interactions. The latter mainly contains dispersion, short-range repulsion, and charge transfer. In the presented calculations both effects are

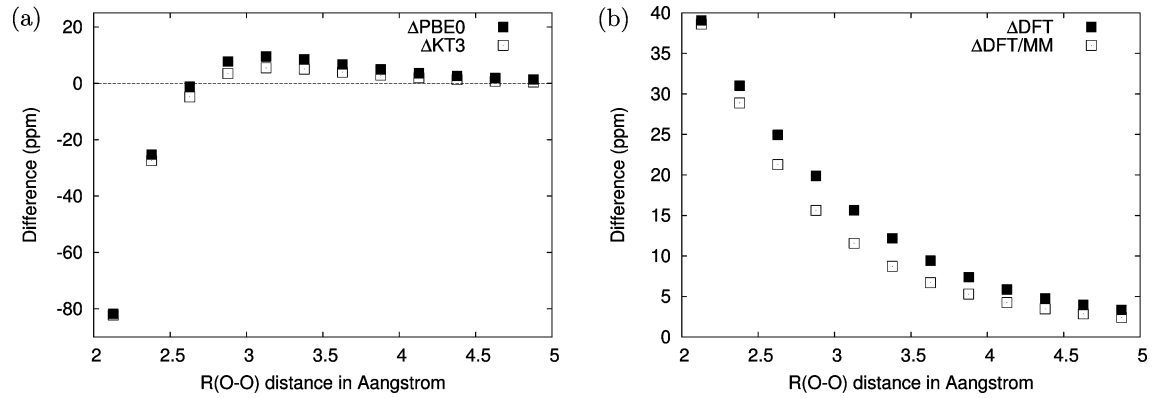

Figure 9. (a) The nonelectrostatic contribution to the $\sigma(^{17}O)$ in formaldehyde due to hydrogen bonding. $\Delta F = \sigma^F - \sigma^{F/MM}$ ($F =$ PBE0,KT3). (b) The difference between the (absolute) $\sigma(^{17}O)$ as calculated using either PBE0 and KT3 (ΔDFT) or the corresponding difference calculated using PBE0/MM and KT3/MM (ΔDFT/MM).

included in the quantum mechanical calculations on the cluster (supermolecule). It is, however, possible to treat only formaldehyde using quantum mechanics and describe the presence of the water molecules in an effective manner. In the following we will compare the results of such a hybrid quantum-classical approach, in which only electrostatic interactions are accounted for, with the supermolecular results. Thereby, we are in a position to estimate the relative importance of either electrostatic or nonelectrostatic intermolecular effects. In the hybrid quantum-classical approach, generally referred to as the DFT/MM model, we describe each water molecule by assigning partial point charges to the nuclei, and in addition we include an electric polarizability at the water oxygen site. The latter gives rise to induction (many-body) effects, i.e., we do *not* assume a pairwise interaction model. The theoretical and implementational aspects of the DFT/MM model have been detailed in ref 5 as well as the ability to calculate origin independent magnetic properties.[36] Different approaches could be used for the derivation of the water molecule parameters describing the electrostatic interactions. For example, partial charges could be calculated using the supermolecule. In this case no polarizability should be assigned to the water molecules since the effect of polarization by formaldehyde is automatically reflected in the charges. However, in such an approach, due to charge transfer between water and formaldehyde, the preceding DFT/MM calculation would generally involved partially charged water molecules. Therefore, we use in the DFT/MM calculation a well-defined water potential.[37] In Figure 9(a) we show the effect of mainly nonelectrostatic contributions to $\sigma(^{17}O)$ calculated using either PBE0 or KT3. For each *xc* functional we have subtracted from the supermolecular prediction of $\sigma(^{17}O)$ the electrostatic component obtained from DFT/MM calculations. Figure 9(a) clearly shows that for short hydrogen bond distances the effect of nonelectrostatic contributions becomes significant. This has previously been discussed by Peralta et al.[38] In addition we observe that the two *xc* functionals describe in a qualitative manner the nonelectrostatic component very similar. This indicates that the difference between the performance of the PBE0 and KT3 *xc* functionals with respect to CCSD(T) predictions (Figure 7) is mainly due to a different treatment of the electrostatic effects by the two *xc* functionals. Further proof for this is found in Figure 9(b) where the differences are shown between the PBE0 and KT3 results for (absolute) $\sigma(^{17}O)$ calculated using either the supermolecular or the quantum-classical approach. From Figure 9(b) it is evident that accounting only for the electrostatic intermolecular interaction effects (DFT/MM) reproduces qualitatively the differences between the PBE0 and KT3 results as obtained from the supermolecular (DFT) calculations.

IV. Discussion and Conclusions

In this paper we have presented the first systematic investigation of the shifts in nuclear magnetic resonance shielding constant due to hydrogen bonds using either the series of wave function based methods HF, MP2, CCSD, and CCSD(T) or DFT employing the B3LYP, PBE0, or KT3 *xc* functionals. We have considered the water dimer and formaldehyde in complex with two water molecules. For these small prototype hydrogen-bonded molecular systems we have presented a systematic study of the effect of various electronic structure methods on the NMR isotropic shieldings. We have especially focused on the performance of the DFT based methods as compared to the corresponding results derived using CCSD(T). The absolute NMR shielding constants are found to be very dependent on both the choice of the many-body electronic structure method and the basis set used in the calculations. For example we fail to observe a basis set convergence for $\sigma(^{17}O)$ in isolated formaldehyde even when using a basis set of aug-cc-pV5Z size and quality. However, the shift in the NMR shielding constants due to complexation with two water molecules shows a relatively fast basis set convergence which is attributed to a cancellation of errors. While the DFT methods perform reasonably in accounting for the shift in the ^{1}H (water) and ^{13}C (formaldehyde) NMR shielding constants due to complexation, less satisfactory results are obtained for the ^{17}O NMR shielding constants. Especially in the case of formaldehyde complexed with two hydrogen-bonding water molecules we find, using either B3LYP or PBE0, significantly too large results as compared to CCSD(T). This overestimation is, however, even more severe when using a HF description of the molecular system. On the other hand, the error introduced by using MP2 is of the same magnitude as that of B3LYP/PBE0 but of opposite sign. In contrast to these failures, the KT3 *xc*

functional is found to provide very accurate results for both the absolute and hydrogen bond shifted ^{17}O NMR shielding constants. Also, when considering intermolecular distortions, KT3 performs reasonably as compared to CCSD(T) and in any case completely outperforms B3LYP and PBE0. This fact is very important when considering calculations of NMR shielding constants based on combined quantum mechanical and statistical methods, where it is mandatory that the NMR shielding constants derived from different solute−solvent configurations are of similar quality, i.e., that the error in the property calculations does not fluctuate between individual calculations.

Even though the molecular systems under scrutiny in this study are small, they represent model systems for more complex or larger samples, for example for acetone or other carbonyl compounds solvated by water. Therefore, our conclusions are of significant importance for the benchmarking of solvent models for quantitative NMR predictions. Recently many popular solvent models, based on either an implicit or explicit description of the solvent, employ DFT. But in fact very little is known about the performance of DFT versus correlated wave function descriptions for solute−solvent interactions. Within this context, the use of DFT has been benchmarked by performing MP2 calculations. This is for example the case in refs 39 and 40, which concern combined quantum mechanics/molecular mechanics or combined quantum mechanics/polarizable continuum model calculations of NMR shielding constants of either formaldehyde or acetone in liquid water. In these studies, DFT was found to give good results for the solvent shift in the ^{17}O NMR shielding constant, particularly, when employing a solvent model which includes electronic polarization explicitly. MP2, on the other hand, was found to underestimate the shifts due to hydrogen bonding. Based on the findings in the present study, part of the success of the theoretical predictions presented in refs 39 and 40 may be attributed to the use of *xc* functionals which artificially overestimate the effect of the solvent on the studied molecular properties. The use of MP2, on the other hand, leads to a severe underestimation of the shifts which, according to the findings presented in this work, is directly attributed to the intrinsic performance of the MP2 model. The overall good agreement between theory and experiment obtained in the DFT based simulations in refs 39 and 40 may on these grounds partly be attributed to error cancellations due to (i) the use of *xc* functionals which overestimate the effect of the solvent, (ii) the use of inaccurate force-fields in the molecular dynamics and combined quantum mechanics/molecular mechanics calculations, and (iii) the neglect of differential zero-point vibrational corrections.[41]

Acknowledgment. The authors thank the Danish Center for Scientific Computing (DCSC) for computational resources. J.K. acknowledges support from the Villum Kann Rasmussen Foundation (Denmark). K.V.M. thanks Forskningsrådet for Natur og Univers (FNU) and the EU network NANOQUANT for support. SPAS thanks Forskningsrådet for Natur og Univers (FNU) and the Carlsberg Foundation.

References

(1) Jeffrey, G. A.; Saenger, W. *Hydrogen bonding in biological structures;* Springer-Verlag: Berlin, 1991.

(2) Steiner, T. *Angew. Chem., Int. Ed.* **2002**, *41*, 48.

(3) Ireta, J.; Neugebauer, J.; Scheffler, M. *J. Phys. Chem. A* **2004**, *108*, 5692.

(4) MacDonald, J. C.; Whitesides, G. M. *Chem. Rev.* **1994**, *94*, 2383.

(5) Nielsen, C. B.; Christiansen, O.; Mikkelsen, K. V.; Kongsted, J. *J. Chem. Phys.* **2007**, *126*, 154112.

(6) Becke, A. D. *J. Chem. Phys.* **1993**, *98*, 5648.

(7) Ernzerhof, M.; Scuseria, G. E. *J. Chem. Phys.* **1999**, *110*, 5029.

(8) Adamo, C.; Barone, V. *J. Chem. Phys.* **1999**, *110*, 6158.

(9) Keal, T. W.; Tozer, D. J. *J. Chem. Phys.* **2004**, *121*, 5654.

(10) Auer, A. A.; Gauss, J.; Stanton, J. F. *J. Chem. Phys.* **2003**, *118*, 10407.

(11) Parker, L. L.; Houk, A. R.; Jensen, J. H. *J. Am. Chem. Soc.* **2006**, *128*, 9863.

(12) Krishna, N. R.; Berliner, L. J, *Biological Magnetic Resonance*; Kluwer/Plenum: New York, 1998−2003; Vol. 16−17, p 20.

(13) Kussmann, J.; Ochsenfeld, C. *J. Chem. Phys.* **2007**, *127*, 054103.

(14) Helgaker, T.; Jaszunski, M.; Ruud, K. *Chem. Rev.* **1999**, *99*, 293.

(15) Gauss, J.; Stanton, J. F. *J. Chem. Phys.* **1996**, *104*, 2574.

(16) Gauss, J.; Stanton, J. F. *J. Chem. Phys.* **1995**, *102*, 251.

(17) Gauss, J.; Stanton, J. F. *J. Chem. Phys.* **1995**, *103*, 3561.

(18) Gauss, J. *Chem. Phys. Lett.* **1992**, *191*, 614.

(19) Cheeseman, J. R.; Trucks, G. W.; Keith, T. A.; Frisch, M. J. *J. Chem. Phys.* **1996**, *104*, 5497.

(20) Lee, A. M.; Handy, N. C.; Colwell, S. M. *J. Chem. Phys.* **1995**, *103*, 10095.

(21) Malkin, V. G.; Malkina, O. L.; Salahub, D. R. *Chem. Phys. Lett.* **1993**, *204*, 80.

(22) Helgaker, T.; Wilson, P. J.; Amos, R. D.; Handy, N. C. *J. Chem. Phys.* **2000**, *113*, 2983.

(23) Ligabue, A.; Sauer, S. P. A.; Lazzeretti, P. *J. Chem. Phys.* **2007**, *126*, 154111.

(24) Kendall, R. A.; Dunning, T. H.; Harrison, R. J. *J. Chem. Phys.* **1992**, *96*, 6796.

(25) Angeli, C.; Bak, K. L.; Bakken, V.; Christiansen, O.; Cimiraglia, R.; Coriani, S.; Dahle, P.; Dalskov, E.; Enevoldsen, T.; Fernandez, B.; Hättig, C.; Hald, K.; Heiberg, H.; Helgaker, T.; Hettema, H.; Jensen, H. J. A.; Jonsson, D.; Jørgensen, P.; Kirpekar, S.; Klopper, W.; Kobayashi, R.; Koch, H.; Ligabue, A.; Lutnæs, O. B.; Mikkelsen, K. V.; Norman, P.; Olsen, J.; Packer, M. J.; Pedersen, T. B.; Rinkevicius, Z.; Rudberg, E.; Ruden, T. A.; Ruud, K.; Salek, P.; Sanchez de Merás, A.; Saue, T.; Sauer, S. P. A.; Schimmelpfennig, B.; Sylvester-Hvid, K. O.; Tayler, P. R.; Vahtras, O.; Wilson, D. J.; Ågren, H. *Dalton, a molecular electronic structure program; Release 2.0*; 2005. See http://www.kjemi.uio.no/software/dalton/dalton.html ed.

(26) Aces II Mainz-Austin-Budapest version. Stanton, J. F.; Gauss, J.; Watts, J. D.; Szalay, P. G.; Bartlett, R. J. with contributions from Auer, A. A.; Bernholdt, D. B.; Christiansen, O.; Harding, M. E.; Heckert, M.; Heun, O.; Huber, C.; Jonsson, D.; Jusélius, J.; Lauderdale, W. J.; Metzroth, T.; Michauk, C.; Price, D. R.; Ruud, K.; Schiffmann, F.; Tajti, A.; Varner, M. E.; Vázquez, J. and the integral packages: Molecule (Almlöf, J.; Taylor, P. R.), Props (Taylor, P. R.), and Abacus (Helgaker, T.; Jensen, H. J. A.; Jørgensen, P.; Olsen, J.). See http://www.aces2.de.

(27) Stanton, J. F.; Gauss, J.; Watts, J. D.; Lauderdale, W. J.; Bartlett, R. J. *Int. J. Quantum Chem. Symp.* **1992**, *26*, 879.

(28) Boys, S. F.; Bernardi, F. *Mol. Phys.* **1970**, *19*, 553.

(29) London, F. *J. Phys. Radium* **1937**, *8*, 397.

(30) Hameka, H. F. *Rev. Mod. Phys.* **1962**, *34*, 87.

(31) Ditchfield, R. *Mol. Phys.* **1974**, *27*, 789.

(32) Wolinski, K.; Hinton, J. F.; Pulay, P. *J. Am. Chem. Soc.* **1990**, *112*, 8251.

(33) Helgaker, T.; Jørgensen, P. *J. Chem. Phys.* **1991**, *95*, 2595.

(34) Karadakov, P. B. *J. Mol. Struct.* **2002**, *602*−*603*, 293.

(35) Wu, A.; Cremer, D.; Gauss, J. *J. Phys. Chem. A* **2003**, *107*, 8737.

(36) Kongsted, J.; Nielsen, C. B.; Mikkelsen, K. V.; Christiansen, O.; Ruud, K. *J. Chem. Phys.* **2007**, *126*, 034510.

(37) Ahlström, P.; Wallqvist, A.; Engström, S.; Jönnson, B. *Mol. Phys.* **1989**, *68*, 563.

(38) Peralta, J. E.; Ruiz de Azua, M. C.; Contreras, R. H. *J. Mol. Struct. (Theochem*) **1999**, *491*, 23.

(39) Pavone, M.; Brancato, G.; Morelli, G.; Barone, V. *Chem. Phys. Chem.* **2006**, *7*, 148.

(40) Aidas, K.; Møgelhøj, A.; Kjær, H.; Nielsen, C. B.; Mikkelsen, K. V.; Ruud, K.; Christiansen, O.; Kongsted, J. *J. Phys. Chem. A* **2007**, *111*, 4199.

(41) Kongsted, J.; Ruud, K. *Chem. Phys. Lett.* **2007**, doi: 10.106/j.cplett.2007.12.008.

CT700285J